TRAFFIC RECONSTRUCTION USING AUTONOMOUS VEHICLES *

MARIA LAURA DELLE MONACHE,[†], THIBAULT LIARD[‡], BENEDETTO PICCOLI[§], RAPHAEL STERN[¶], AND DAN WORK[‖]

Abstract. We consider a partial differential equation - ordinary differential equation system to describe the dynamics of traffic flow with autonomous vehicles. In the model the bulk flow is represented by a scalar conservation law, while each autonomous vehicle is described by a car following model. The autonomous vehicles act as tracer vehicles in the flow and collect measurements along their trajectories to estimate the bulk flow. The main result is to both prove theoretically and show numerically how to reconstruct the correct traffic density using only the measurements from the autonomous vehicles.

Key words. Scalar conservation laws, PDE-ODE systems, Density reconstruction, Traffic flow models

AMS subject classifications. 35L65; 90B20

1. Introduction.

In recent years Autonomous Vehicles (briefly AVs) have been tested on urban and highway networks and appear to be the technology with the highest chance of disruptive changes for the future of traffic monitoring and management. Traffic monitoring already underwent a major disruption when the use of fixed location sensors and cameras were supplemented by Lagrangian sensing via mobile phones and other devices. AVs will further contribute to this disruption by acting as highly reliable moving sensors equipped with high-tech on-board devices that can record local traffic conditions. The aim of this paper is to show how a small number of AVs immersed in bulk traffic are capable of monitoring the traffic density along a road without any other data sources. Mathematically we rely on a coupled Ordinary Differential Equation Partial Differential Equation (ODE-PDE) model representing the combined evolution of bulk traffic density and the positions of AVs.

Let us start providing some background on traffic estimation. The field of traffic reconstruction began with experiments in the Lincoln Tunnel in New York City [14, 25]. Since then, the field has seen significant development in terms of the modeling employed as well as the estimation algorithms used to integrate realtime data [26, 27, 18]. For a recent summary of the developments of model based traffic estimation, see [20, 11]. More recently there has been an interest to explore estimation in Lagrangian coordinates [28, 15] where sensors are embedded in the traffic flow instead of being placed at fixed locations in the infrastructure. For example, the *Mobile Century* project [16, 27] used GPS data from mobile phones as measurements for Lagrangian traffic state estimation. Such Lagrangian traffic state estimation techniques have often relied on GPS data from the vehicles [27, 13], and more recently from spacing

*Submitted to the editors DATE.

Funding: The work of the first author was supported by the IDEX-IRS 2018 project "MAVIT-Modeling autonomous vehicles in traffic flow" and by the support of Inria associated team "MEMENTO."" This material is based upon work supported by the National Science Foundation under grants CNS-1837652 (D.W.) and CNS-1837481 (B.P.).

[†]Univ. Grenoble Alpes, Inria, CNRS, Grenoble INP, GIPSA-Lab, 38000 Grenoble, France (ml.dellemonache@inria.fr).

[‡]Univ. Grenoble Alpes, Inria, CNRS, Grenoble INP, GIPSA-Lab, 38000 Grenoble, France (thibault.liard@inria.fr).

[§]Rutgers University-Camden, NJ, USA (piccoli@camden.rutgers.edu).

[¶]Vanderbilt University, TN, USA (stern5@illinois.edu).

[‖]Vanderbilt University, TN, USA (dan.work@vanderbilt.edu).

measurements from on-board sensors [21]. Since AVs are also highly instrumented vehicles, they may be able to provide additional measurements that can further improve traffic estimation.

We now briefly describe the mathematical aspects of the paper. One of the most widely used macroscopic models in traffic is the celebrated Lighthill-Whitham-Richards model [17, 19], which consists of a single conservation law for the traffic density. Particle trajectories for the model represent car trajectories and can be constructed using solutions to discontinuous ODEs, see [6]. Considering together the traffic density and a small number of particle trajectories gives rise to a partially coupled PDE-ODE system, where the ODEs depend on the PDE solution but not vice versa [5]. Alternatively, in [8] the authors introduced scalar conservation laws with moving flux constraints. The latter represent a moving bottleneck, which in turn may correspond to a vehicle such as a truck or an AV driving differently than the bulk traffic. The model [8] is a completely coupled PDE-ODE model. Here we assume that the AVs do not influence traffic by their driving, and therefore we consider the partially coupled model.

Our problems can be formulated as control problems. We consider a stretch of road with incoming and outgoing traffic and a small number of AVs entering the road that are able to measure the density along their trajectories. The aim is to control the speed of each AV (compatibly with the traffic conditions) in such a way that the collected data allows for a complete reconstruction of the traffic density along the road after a certain time. This corresponds to generating moving boundaries (by controlling the AVs), so that the solution to the conservation law compatible with the measured data along such boundaries is unique. This problem is new, and can be addressed using typical tools from the theory of conservation laws. More specifically, initial-boundary value problems are well understood [10, 2, 22, 23] and semigroup of solutions are constructed via wave-front tracking [9, 1, 3]. Using these results, we first show that it is possible to define explicitly a time horizon such that, if such horizon is finite, then complete traffic reconstruction is possible for all times after such horizon. Moreover, the main result (Theorem 3.2) determines all initial conditions which give rise to the observed density at the time horizon. The result is then extended to the case of a ring road.

We then turn to the attention to the problem of reconstructing the density from the measurements from AVs (which is proved possible by the main Theorem 3.2). Again using the wave-front tracking approach, we define an algorithm which takes the the data from AVs as input and returns the reconstructed traffic density as output. Since we use wave-front tracking, our solution is piecewise constant in time-space and the trajectory of each AV has a piecewise constant speed (changing only at points where the trajectory intersects with a wave). Therefore, all data (including each AV trajectory and the measurements along it) are finite dimensional and the algorithm can be implemented on a regular personal computer. We are then able to present various numerical experiments of traffic reconstruction along a stretch of road.

The paper is organized as follows. In Section 2, we briefly introduce the coupled ODE-PDE model before describing the main theoretical results in Section 3. In Section 4 a numerical scheme to estimate the traffic density from the AVs is introduced, and in Section 5 the scheme is applied to numerical experiments. Section 6 discusses possible extensions of the work.

2. Model description. By detecting the local density via sensors of autonomous vehicles, we want to reconstruct the density at a certain time T and on a portion of

a road. In order to do this, we need to be able to describe the traffic dynamics and reconstruct the density starting from the measurements of the autonomous vehicles. Let us consider a stretch of road $\mathbb{R}$ with mixed traffic, i.e., partly human-piloted traffic and partly autonomous vehicles. This situation can be modeled with a PDE-ODE system consisting of a scalar conservation law accounting for the human-piloted traffic and a system of ODEs describing the dynamics of the autonomous vehicles. From a mathematical point of view this means that the main bulk of human-piloted traffic is described with the *Lighthill-Whitham-Richards* (LWR) macroscopic model, [17, 19], i.e. the mass conservation equation

$$\partial_t \rho + \partial_x f(\rho) = 0, \qquad (t, x) \in \mathbb{R}^+ \times \mathbb{R}. \tag{2.1}$$

In (2.1), $\rho = \rho(t, x) \in [0, \rho_{\max}]$ is the mean traffic density, $\rho_{\max}$ is the maximal density and the flux function $f : [0, \rho_{\max}] \to \mathbb{R}^+$ is given by the following flux-density relation:

$$f(\rho) = \rho v(\rho), \tag{2.2}$$

where $v(\rho)$ is a smooth decreasing function denoting the mean traffic speed. We will assume for simplicity that the following hold:

(A1) $\rho_{\max} = 1$;
(A2) $f(0) = f(1) = 0$;
(A3) f is a strictly concave function.

Assumptions (A2), (A3) ensure the uniqueness of a maximum point of the flux function at a critical density $\rho_{\rm cr} \in [0, 1]$.
A typical example of a flux function for the LWR model is given in Figure 1.

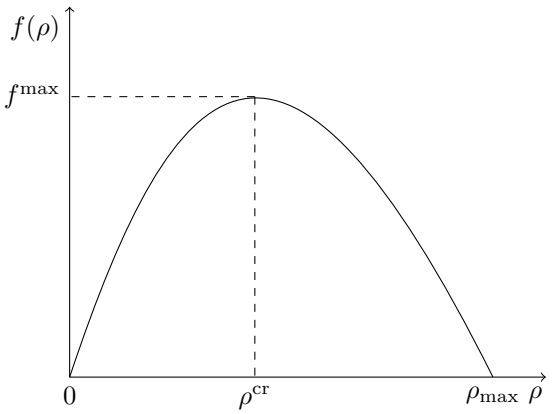

Fig. 1: The flux function (2.2) is commonly referred to as fundamental diagram in the transportation literature.

The conservation law (2.1) with initial density $\rho_0(\cdot) \in BV(\mathbb{R}, [0, 1]) \cap L^1(\mathbb{R}, [0, 1])$ admits an entropy solution $\rho \in C^0\left([0, +\infty[; \mathbf{L}^1 \cap BV(\mathbb{R}; [0, 1])\right)$, see [4]. For every $t \in [0, \infty)$, $\rho(t, \cdot) \in BV(\mathbb{R}; [0, 1])$, thus it admits right and left limits: $\rho(t, x_0+) := \lim_{x \to x_0, x > x_0} \rho(t, x)$ and $\rho(t, x_0-) := \lim_{x \to x_0, x < x_0} \rho(t, x_0)$.

Let us briefly recall the concept of a Riemann problem and its solution. For (2.1) a Riemann type initial data is given by

$$\rho_0(x) = \begin{cases} \rho_L, & \text{if} \quad x < 0, \\ \rho_R, & \text{if} \quad x > 0. \end{cases} \tag{2.3}$$

Entropic self-similar solutions to the Riemann problem are defined as:

- If $\rho_L < \rho_R$: a shock wave (ρ_L, ρ_R) traveling with speed given by the Rankine-Hugoniot condition $\sigma(\rho_L, \rho_R) = \frac{f(\rho_L)-f(\rho_R)}{\rho_L-\rho_R}$ namely:

$$\rho(t,x) = \begin{cases} \rho_L, & \text{if } x < \sigma(\rho_L, \rho_R)t, \\ \rho_R, & \text{if } x > \sigma(\rho_L, \rho_R)t. \end{cases}$$

- If $\rho_L > \rho_R$: a rarefaction wave (ρ_L, ρ_R) namely:

$$\rho(t,x) = \begin{cases} \rho_L, & \text{if } x < f'(\rho_L)t, \\ (f')^{-1}(\frac{x}{t}), & \text{if } f'(\rho_L)t < x < f'(\rho_R)t, \\ \rho_R, & \text{if } x > f'(\rho_R)t. \end{cases}$$

We will also make extensive use of the theory of generalized characteristics. Since ρ is, in general, discontinuous in the space variable, classical characteristics must be replaced by generalized ones, which solve a differential inclusion, instead of an ordinary differential equation. We refer the reader to [7] for details. In the Appendix A.1 we provide a brief overview. We consider that along the road at a certain time t there are N autonomous vehicles that are able to detect the local vehicle density via sensors. We assume that we can collect their information starting at a position $x = \alpha \in \mathbb{R}$ and at time $t \geqslant 0$. The N autonomous vehicles are distributed in two groups N_1, $N_2 + 1$ in the following way (see Figure 2):

- N_1 vehicles enter the stretch of road considered at time $t > 0$ via an entrance ramp positioned at $x = \alpha$.
- $N_2 + 1$ vehicles are located at position $x \geqslant \alpha$ at time $t = 0$.

All the autonomous vehicles are modeled via the following ODE-system:

$$\begin{cases} \dot{y}_i(t) = u_i(\rho(t, y_i(t)+)) & t \in [t_i, +\infty), i = -N_1, \cdots, N_2, \\ y(t_i) = y_0^i & i = -N_1, \cdots, N_2. \end{cases} \tag{2.4}$$

Above, u_i is a decreasing function verifying that

$$\begin{cases} u_i(\rho) > f'(\rho), & \text{if } \rho > 0, \\ u_i(\rho) = f'(\rho), & \text{if } \rho = 0. \end{cases} \tag{2.5}$$

The autonomous vehicles move faster than every wave-front allowing the existence of solutions to (2.4) in Carathéodory sense, that is to say for $t \in (t_i, +\infty)$, (2.4) holds. If $i \in \{-N_1, \cdots, -1\}$, the vehicles enter the road $[\alpha, \infty)$ at time $t_i > 0$ in a position $y_0^i = \alpha$. If $i \in \{0, \cdots, N_2\}$, the vehicles are already in the stretch of road $[\alpha, \infty)$, therefore $t_i = 0$ and $\alpha \leqslant y_0^i$.

The Cauchy problem that describes the traffic dynamics is then:

$$\begin{cases} \partial_t \rho + \partial_x(f(\rho)) = 0, & (t,x) \in \mathbb{R}^+ \times \mathbb{R}, \\ \rho(0,x) = \rho_0(x), & x \in \mathbb{R}, \\ \dot{y}_i(t) = u_i(\rho(t, y_i(t)+))), & t > t_i, i = -N_1, \cdots, N_2, \\ y_i(t_i) = y_0^i, & i = -N_1, \cdots, -1. \end{cases} \tag{LWR-AVs}$$

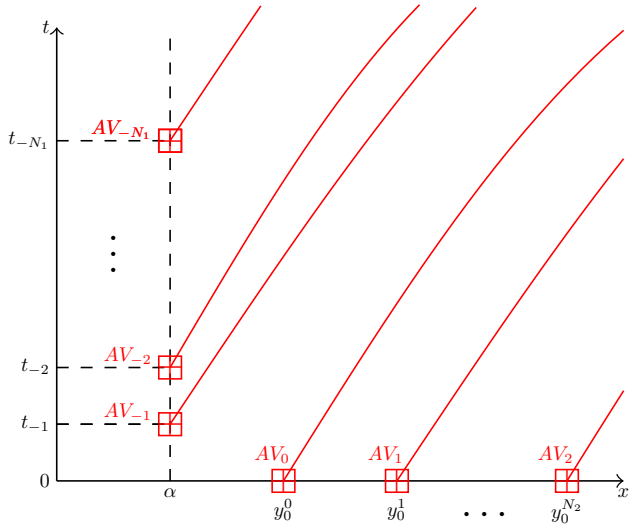

Fig. 2: AVs along the road at a certain time t.

with

$$\begin{cases} t_{-N_1} > \cdots > t_{-1} > 0 = t_0 = \cdots = t_{N_2}, \\ y_0^{-N_1} = \cdots = y_0^{-1} = \alpha \leqslant y_0^0 < \cdots < y_0^{N_2}. \end{cases}$$

Above, $\rho_0(\cdot) \in BV(\mathbb{R},[0,1]) \cap L^1(\mathbb{R},[0,1])$ and, for every $i \in \{-N_1, \cdots, N_2\}$, $y_0^i(\cdot) \in \mathbb{R}$ are the initial conditions. From [6, 8], the Cauchy problem admits an entropy solution $\rho \in C^0\left([0,+\infty[;\mathbf{L}^1 \cap BV(\mathbb{R};[0,1])\right)$ and for every $i \in \{-N_1, \cdots, N_2\}$, a Carathéodry solution $y_i \in W^{1,1}([t_i,+\infty),\mathbb{R})$.

Our goal is to find a time T at which it is possible to reconstruct the true density ρ between two autonomous vehicles based only on the measured local density of each AV.

3. Main results. Let us first introduce the following operators that aim at simplifying the notation of the proofs:

- $S_t : L^1(\mathbb{R}) \cap BV(\mathbb{R},[0,1]) \mapsto L^1(\mathbb{R}) \cap BV(\mathbb{R},[0,1])$ is a L^1-Lipschitz semigroup defined by $S_t(\rho_0) = \rho(t,\cdot)$ s.t. ρ is the solution of

$$\text{(LWR)} \qquad \begin{cases} \partial_t \rho + \partial_x(f(\rho)) = 0, & (t,x) \in \mathbb{R}^+ \times \mathbb{R}, \\ \rho(0,x) = \rho_0(x), & x \in \mathbb{R}. \end{cases}$$

- $\Gamma : BV(\mathbb{R},[0,1]) \cap L^1(\mathbb{R}) \to (C^0(\mathbb{R}_+, BV(\mathbb{R},[0,1]) \cap L^1(\mathbb{R}))^2)^N$ defined by $\Gamma(\rho_0) = (\rho(\cdot, y_i(\cdot)\pm))_{i\in\{-N_1,\cdots,N_2\}}$ where (ρ, y_i) is the solution of (LWR-AVs) with initial data ρ_0 and $N := N_2 + N_1 + 1$ is the number of autonomous vehicles. $\Gamma_i(\cdot)$ denotes the i^{th} component of $\Gamma(\cdot)$.

Let $\bar{\rho}_0 \in BV(\mathbb{R},[0,1]) \cap L^1(\mathbb{R})$ be some unknown initial data. For $i \in \{-N_1, \cdots, N_2 - 1\}$, by collecting only $(\Gamma_i(\bar{\rho}_0), \Gamma_{i+1}(\bar{\rho}_0)) := (\rho(\cdot, y_i(\cdot)\pm), \rho(\cdot, y_{i+1}(\cdot)\pm))$ via sensors

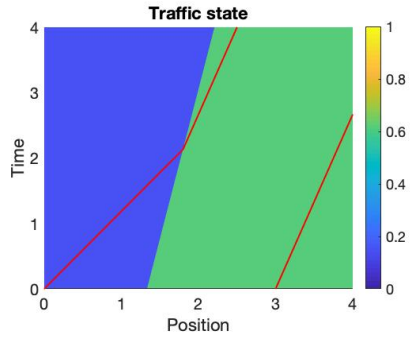

(a) $\rho_0(x) = 0.16\mathbb{1}_{(-\infty,1.33)} + 0.63\mathbb{1}_{(1.33,\infty)}$ with two autonomous vehicles positioned at $y_0^1 = 0$ and $y_0^2 = 3$.

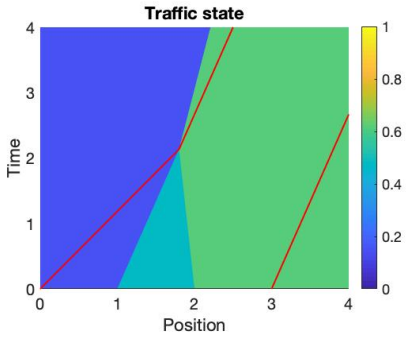

(b) $\rho_0(x) = 0.16\mathbb{1}_{(-\infty,1)} + 0.47\mathbb{1}_{(1,2)} + 0.63\mathbb{1}_{(2,\infty)}$ with two autonomous vehicles positioned at $y_0^1 = 0$ and $y_0^2 = 3$.

Fig. 3: Illustration of Example 1: Γ is not a surjective function.

of the i^{th} autonomous vehicle and the $(i+1)^{\text{th}}$ autonomous vehicle, we want to reconstruct $S_{T_i}(\bar\rho_0)(x)$ for every $x \in [y_i(T_i), y_{i+1}(T_i)]$ at a certain time $T_i \geqslant 0$. For every $i \in \{-N_1, \cdots, N_2\}$ the trajectory of the i-th autonomous vehicle is described by (2.4).

Example 1 shows that we cannot reconstruct the solution at any time. Theorem 3.2 gives a way to find the reconstruction time T.

EXAMPLE 1. *Assume that $f(\rho) = \rho(1-\rho)$ and two autonomous vehicles are deployed at $(0,0)$ and at $(3,0)$ respectively with speed $u_1(\rho) = u_2(\rho) = 1-\rho$ (see Figure 3). Let $\rho_0 < \rho_1 < \rho_2$ and $\frac{1}{\rho_1} = \frac{1}{\rho_2 - \rho_0}$. We introduce the two following initial densities*

$$\bar\rho_0 = \rho_0 \mathbb{1}_{(-\infty, 1+\frac{\rho_2-\rho_1}{\rho_2-\rho_0})} + \rho_2 \mathbb{1}_{(1+\frac{\rho_2-\rho_1}{\rho_2-\rho_0}, \infty)},$$

$$\tilde\rho_0 = \rho_0 \mathbb{1}_{(-\infty,1)} + \rho_1 \mathbb{1}_{(1,2)} + \rho_0 \mathbb{1}_{(2,\infty)}.$$

We have $\Gamma(\tilde\rho_0) = \Gamma(\bar\rho_0)$ and for every $t \in [0, \frac{1}{\rho_2-\rho_1})$, $S_t(\tilde\rho_0) \neq S_t(\bar\rho_0)$. Thus, we cannot reconstruct $\rho(t,\cdot)$ for every $t \in [0, \frac{1}{\rho_2-\rho_1})$ by collecting only $\Gamma(\bar\rho_0) = \Gamma(\tilde\rho_0)$ via the sensors of both autonomous vehicles.

We define the multifunction $\varphi_i : [t_i, +\infty) \mapsto \mathcal{P}(\mathbb{R})$, where $\mathcal{P}(\mathbb{R})$ is the set of subsets of $\mathbb{R}$, as follows:

$$\varphi_i(t) = [f'(\rho(t, y_i(t)-))(t_{i+1} - t) + y_i(t), f'(\rho(t, y_i(t)+))(t_{i+1} - t) + y_i(t)]. \tag{3.1}$$

Remark 3.1. The minimal backward characteristic $s \mapsto f'(\rho(t, y_i(t)-))(s-t) + y_i(t)$ and the maximal backward characteristic $s \mapsto f'(\rho(t, y_i(t)+))(s-t) + y_i(t)$ from the point $(t, y_i(t))$ bound the domain of dependence of $\rho(t, y_i(t))$ (see the shaded region in Figure 4).

THEOREM 3.2. *Let $\bar\rho_0 \in BV(\mathbb{R}, [0,1]) \cap L^1(\mathbb{R})$. For every $i \in \{-N_1, \cdots, N_2 - 1\}$, the i^{th} autonomous vehicle starts at time t_i in the position y_0^i and its trajectory is*

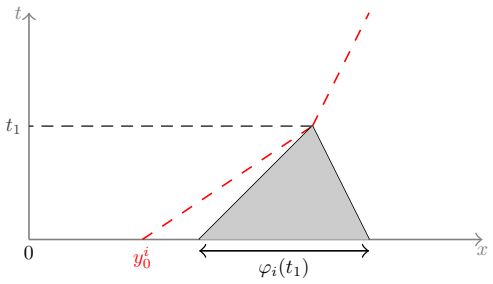

Fig. 4: Representation of the domain of dependence by backward characteristics: $\varphi_i(t_1)$ with $t_1 > 0$ (shaded region). The trajectory of the i^{th} autonomous vehicle is represented by dashed red line.

described by (2.4). *Moreover, we impose that* u_i *verifies* (2.5). *Let* $T_i \in [t_i, +\infty) \cup \{\infty\}$ *be defined by*

$$T_i := \sup_{\{T \in \mathbb{R}_+ / y_0^{i+1} \in \varphi_i(T)\}} T. \tag{3.2}$$

If $T_i < \infty$ *then for every* $\rho_0 \in \Gamma^{-1}(\Gamma(\bar{\rho}_0))$, $S_{T_i}(\rho_0)(x) = S_{T_i}(\bar{\rho}_0)(x)$, *for every* $i \in \{-N_1, \cdots, N_2\}$ *and for almost every* $x \in [y_i(T_i), y_{i+1}(T_i)]$ *with* (y_i, y_{i+1}) *solution of* (2.4).

Example 2. *Assume that* $f(\rho) = \rho(1-\rho)$ *and two autonomous vehicles are deployed on the road at* $(0, y_0^1)$ *and at* $(0, y_0^2)$ *with speed* $u_1(\rho) = u_2(\rho) = 1 - \rho$. *Assume that the first autonomous vehicle collects only the density* ρ_1, *that is to say* $\rho(t, y_1(t)) = \rho_1$ *for every* $t \in \mathbb{R}_+$. *Then, we have, for every* $t \in \mathbb{R}_+$,

$$\begin{aligned} \varphi_1(t) &= -f'(\rho_1)t + (1-\rho_1)t + y_0^1, \\ &= \rho_1 t + y_0^1, \end{aligned}$$

From (3.2), *we conclude that* $T_1 = \frac{y_0^2 - y_0^1}{\rho_1}$.

In Example 2, $\lim_{\rho_1 \to 0} T_1 = \lim_{\rho_1 \to 0} \frac{y_0^2 - y_0^1}{\rho_1} = \infty$. Theorem 3.3 gives a sufficient condition on the initial density $\bar{\rho}_0$ to have a finite reconstruction time T_i, $i \in \{-N_1, \ldots, N_2 - 1\}$.

Theorem 3.3. *We assume that* $\bar{\rho}_0 \in BV(\mathbb{R}, [0,1]) \cap L^1(\mathbb{R})$ *with the additional property that for every* $x \in \mathbb{R}$, $0 < \rho_{\min} \leqslant \bar{\rho}_0(x) \leqslant \rho_{\max}$. *Then, we have*

$$c_i = \min_{\rho \in [\rho_{\min}, \rho_{\max}]} (u_i(\rho) - f'(\rho)) > 0$$

and for every $i \in \{-N_1, \cdots, N_2\}$,

$$\frac{y_0^{i+1} - y_0^i}{u_i(\rho_{\min}) - f'(\rho_{\max})} + t_{i+1} \leqslant T_i \leqslant \frac{(y_0^{i+1} - y_0^i + f'(\rho_{\min})(t_i - t_{i+1}))}{c_i} \left(1 + \exp\left(\frac{\alpha T V(\rho_0)}{c_i}\right)\right) \tag{3.3}$$

with $\alpha = \sup_{\rho \in [0,1]} f''(\rho)$.

The proofs of Theorem 3.2 and Theorem 3.3 are presented in Appendix A.

Remark 3.4. The reconstruction time T_i in Theorem 3.3, depends on the distance between the initial positions of the AVs. For a fixed road one can estimate the number of AVs needed to guarantee a reconstruction time as function of the road length.

Main ideas of the proof of Theorem 3.2.
Let $\bar\rho_0$ be an unknown initial data. For every time $t > 0$, the i-th AV (denoted by AV_i) measures locally in time the density $\rho(t, y_i(t)\pm)$ and its new speed becomes $u_i(\rho(t, y_i(t)+))$. The trajectory of AV_i is described by (2.4). Since $u_i(\rho) \geqslant f'(\rho)$ for every $\rho \in [0, 1]$, the speed of AV_i is faster than (or equal to) the speed of every discontinuity. At time T_i, defined in (3.2), the AV_i has already interacted with every discontinuity wave coming from $(0, x)$ with $x \in (y_0^i, y_0^{i+1})$ or from (t, α) with $t \in (t_{i+1}, t_i)$. Thus, the solution over $\{(T_i, x) \in \mathbb{R}_+ \times \mathbb{R}/\, y_i(T_i) \leqslant x \leqslant y_{i+1}(T_i)\}$ can be deduced using only the data $\rho(\cdot, y_{i+1}(\cdot)-)$ collected by the AV_{i+1}. Therefore, Theorem 3.2 is proved using the uniqueness of (LWR) defined on $\{(t, x) \in \mathbb{R}_+ \times \mathbb{R}, x < y_{i+1}(t)\}$ with the boundary condition $\rho(\cdot, y_{i+1}(\cdot))$.

A smaller reconstruction time as compared to (3.2) can be found when the speed of AV_i is constant.

LEMMA 3.5. *Let $i \in \{-N_1, \cdots, N_2\}$. We assume that $u_i(\rho) \geqslant f'(\rho)$. Let $T_i > 0$ such that (3.2) holds. If there exists $a \in \mathbb{R}_+$ and $b \in \mathbb{R}_+$ such that $\rho(\cdot, y_i(\cdot))$ is a constant function over $[a, b)$ and $T_i \in [a, b)$ then, for every $\rho_0 \in \Gamma^{-1}(\Gamma(\bar\rho_0))$, $S_a(\rho_0)(x) = S_a(\bar\rho_0)(x)$ for almost every $x \in [y_i(a), y_{i+1}(a)]$ with (y_i, y_{i+1}) the solution of (2.4).*

The proof is deferred to Appendix A.5.

3.1. Extension to ring roads. We consider a ring of length L. By detecting local traffic density via M autonomous vehicles, we want to reconstruct the density on the whole ring at a certain time $T_{\max}$. We consider the following LWR model with periodic boundary conditions

$$\text{(LWR-ring)} \qquad \begin{cases} \partial_t \rho + \partial_x(f(\rho)) = 0, & (t, x) \in \mathbb{R}^+ \times [0, L], \\ \rho(0, x) = \bar\rho_0(x), & x \in [0, L], \\ \rho(t, 0) = \rho(t, L), & t \in \mathbb{R}_+. \end{cases}$$

All the autonomous vehicles are modeled via the following iterative method: $t \in [0, t_i^1) \to y_i(t)$ is solution of

$$\begin{cases} \dot y_i(t) = u_i(\rho(t, y_i(t)+)), & t \in [0, t_i^1), i = 1, \cdots, M \\ y(0) = y_0^i, & i = 1, \cdots, M, \end{cases} \tag{3.4}$$

with $t_i^1 > 0$ is defined as follows: if there exists a time $\bar t > 0$ such that $y_i(\bar t) = L$ then $t_i^1 = \bar t$. Otherwise, we have $t_i^1 = +\infty$. If $t_i^1 \neq +\infty$, $t \in [t_i^1, t_i^2) \to y_i(t)$ is a solution of

$$\begin{cases} \dot y_i(t) = u_i(\rho(t, y_i(t)+)), & t \in [t_i^1, t_i^2), i = 1, \cdots, M \\ y(t_i^1) = 0, & i = 1, \cdots, M, \end{cases} \tag{3.5}$$

where $t_i^2 > t_i^1$ is defined as $t_i^1 > 0$ and so on.

THEOREM 3.6. *Assume $\bar\rho_0 \in BV([0, L], [0, 1]) \cap L^1([0, L])$ with the additional property that for every $x \in [0, L]$, $0 < \rho_{\min} \leqslant \bar\rho_0(x) \leqslant \rho_{\max}$, and let*

$$c = \min_{i \in \{1, \cdots, M\}} \min_{\rho \in [\rho_{\min}, \rho_{\max}]} (u_i(\rho) - f'(\rho)). \tag{3.6}$$

There exists $T_{max} < \infty$ *satisfying*

$$T_{max} \leqslant \max_{i\in\{1,\cdots,M\}} (y_0^{i+1} - y_0^i) \left(\frac{1 + \exp(\frac{\alpha TV(\rho_0)}{c})}{c} \right),$$

such that for every $\rho_0 \in \Gamma^{-1}(\Gamma(\bar{\rho}_0))$, $S_{T_{\max}}(\rho_0)(x) = S_{T_{\max}}(\bar{\rho}_0)(x)$ *for every* $x \in [0, L]$.

The proof of Theorem 3.6 is postponed to Appendix A.6

4. Numerical scheme. The goal of this section is to describe the numerical scheme that is used to reconstruct the density. Our aim is to design a scheme that is able to numerically approximate the conservation law and the autonomous vehicles on a fixed mesh, and use this scheme for the reconstruction algorithm. In the following section we show how to simulate the PDE-ODE system by describing the numerical methods adopted. Then we describe the reconstruction algorithm in detail.

4.1. Construction of the true state (ρ^n, y^n)**.**

4.1.1. Wave-front tracking method for the conservation law. To construct piecewise constant approximate solutions, we adapt the standard Wave-Front Tracking (WFT) method, see for example [4, Chapter 6]. The goal of the wave-front tracking is to approximate and compute the solution of the conservation law. Fix a positive $n \in \mathbb{N}$, $n > 0$ and introduce in $[0, 1]$ the mesh $\mathcal{M}_n = \{\rho_i^n\}_{i=0}^{2^n}$ defined by

$$\mathcal{M}_n = (2^{-n}\mathbb{N} \cap [0, 1]).$$

The WFT method works as follows:

1) Approximate the initial data $\rho_0 \in \mathrm{BV}(\mathbb{R}, [0, 1])$ with piecewise constant functions ρ_0^n such that for every $x \in \mathbb{R}$, $\rho_0^n(x) \in \mathcal{M}_n$.
2) Solve the Riemann problems generated by the jumps $(\rho_0^n(x_i-), \rho_0^n(x_i+))$ for $i = 1, \cdots, N$ where $x_0 < \cdots < x_N$ are the points where ρ_0^n is discontinuous.
3) Piece the solutions together approximating rarefaction waves with fans of rarefaction shocks where the speed of each shock has strength 2^{-n} and is prescribed by the Rankine-Hugoniot condition.
4) The piecewise constant approximate solution ρ^n that is constructed can be prolonged up to the fist time $t_1 > 0$, where the two discontinuities collide. In this case, a new Riemann problem arises and needs to be solved.

4.1.2. Numerical method for the ODE. Let $\rho^n(t, \cdot)$ be the WFT approximate solution associated to ρ_0^n (see subsection 4.1.1). In this section, we describe how to solve the following ODE numerically:

$$\begin{cases} \dot{y}_i^n(t) = u_i(\rho^n(t, y_i^n(t)+)) & t \in [t_i, +\infty], i = -N_1, \cdots, N_2, \\ y(t_i) = y_0^i & i = -N_1, \cdots, N_2. \end{cases} \tag{4.1}$$

Since the solution y_i^n of (4.1) is a continuous piecewise linear function, it is enough to find the points of discontinuity of $\dot{y}_i^n$, denoted by $(t_{i,k}, y_i^{n,k})_{k\in\{1,\cdots,K\}}$.

Step 0. We impose $(t_{i,0}, y_i^{n,0}) = (t_i, y_0^i)$.

Step 1. From $(t_{i,k}, y_i^{n,k})$, we determine the position of the autonomous vehicles $(t_{i,k+1}, y_i^{n,k+1})$ as follows. For the ODE (4.1), we have

$$y_i^{n,k+1} = u_i(\rho^n(t_{i,k}, y_i^{n,k}+)))(t_{i,k+1} - t_{i,k}) + y_i^{n,k},$$

where $t_{i,k+1}$ is the first interaction time between the straight line defined by

$$\{u_i(\rho^n(t, y_i^{n,k}+)))(t - t_{i,k}) + y_i^{n,k}, t > t_{i,k}\},$$

and elements of the set of discontinuity waves of $\rho^n(t, \cdot)$ with $t > t_{i,k}$.

4.2. Reconstruction scheme. In this section we describe in detail the algorithm for the density reconstruction. For simplicity, we drop the index n. We assume that the initial density $\rho_0 : \mathbb{R} \to \mathcal{M}_n$ is a piecewise constant function and ρ is the solution to (LWR) with initial density ρ_0.

Algorithm. Algorithm for the reconstruction of the density between two AVs i and $i + 1$.

Input data:

- Discontinuity points $(t_{i,k})_{k\in\{1,\cdots,K\}}$ of $\dot{y}_i$.
- AV trajectories: $y_i(t_{i,k}) := y_i^k$ and $y_{i+1}(t_{i,k}) := y_{i+1}^k$.
- Densities measured by the AVs $\rho(t_{i,k}, y_i^k\pm))$ and $\rho(t_{i,k}, y_{i+1}^k\pm))$.

Step 0. Impose $t_{i,K+1} = \infty$, $\rho_{i+1,\text{rec}}(t, x) = \rho(t_{i+1}, y_0^{i+1}-)$ for every $(t, x) \in [t_{i+1}, t_{i+1,1}] \times \mathbb{R}$. To avoid misunderstanding, we recall that t_{i+1} is the starting time of AV_i and $t_{i+1,1} > t_{i+1}$ is the first discontinuity point of y_i.

Step 1. Compute the reconstruction density $\rho_{i+1,\text{rec}}(t_{i+1,k}, \cdot)$ at every time $t_{i+1,k}$ only using data collected by the $(i + 1)^{\text{th}}$-autonomous vehicle.
For every $k \in \{1, \cdots, K - 1\}$,

- Solve all Riemann problems at time $t_{i+1,k}$ for (LWR-AVs) associated with

$$\rho_{i+1,\text{rec}}(t_{i+1,k}, \cdot)\mathbb{1}_{(\infty, y_{i+1}(t_{i+1,k}))} + \rho(t_{i+1,k}, y_{i+1}(t_{i+1,k}+))\mathbb{1}_{(y_{i+1}(t_{i+1,k}),\infty)}.$$

- Piece solutions together where the speed of each wave front is prescribed by the Rankine-Hugoniot condition.
- The solution (denoted by $\rho_{i+1,\text{rec}}$) is prolonged until $\min(t_1, t_{i+1,k+1})$ where t_1 is the first time when two wave-fronts interact. If $t_1 \leqslant t_{i+1,k+1}$, the Riemann problems associated with $\rho_{i+1,\text{rec}}(t_1, \cdot)$, which is still a piecewise constant function, can again be approximately solved within the class of piecewise constant functions and so on until $t = t_{i+1,k+1}$.

end
We end our construction by taking the restriction over $\{(t, x) \in \mathbb{R}_+ \times [y_i(t), y_{i+1}(t)]\}$.

Step 2. Compute the reconstruction time T_i only using $(y_i^k, \rho(\cdot, y_i^k(\cdot)\pm))$ and y_0^{i+1}.
For every $k \in \{1, \cdots, K\}$,
if $y_0^{i+1} \in [f'(\rho(t, y_i^k-))(t_i - t_{i,k}) + y_i^k, f'(\rho(t, y_i^{k+1}-))(t_i - t_{i,k+1}) + y_i^{k+1}]$ then $T_i = t_{i,k}$.
end

Output data: $\rho_{i+1,\text{rec}}(T_i, x)$, for every $x \in [y_i(T_i), y_{i+1}(T_i)]$.

Remark 4.1. If we start with a density $\rho_0 \in BV(\mathbb{R}, [0, 1])$, the source of errors in the reconstruction of the true solution only comes from the approximation of $\rho_0 \in BV(\mathbb{R}, [0, 1])$ (step (1) subsection 4.1.1) and the fact that we split a rarefaction wave into a sequence of rarefaction shocks with strength 2^{-n} (step (3) subsection 4.1.1). Thus, the reconstruction procedure presented in Section 4.3 does not create additional

errors. To simplify the numerical results, we will only consider initial data $\rho_0 : \mathbb{R} \to \mathcal{M}_n$ in the next section.

5. Numerical results. Numerical results are simulated using the flux function $f(\rho) = \rho(1-\rho)$ and the speed of each AV_i is $u_i(\rho) = 1-\rho$. Simulations are conducted using the WFT method described above. Rarefaction shocks are approximated as waves with a change in density of $2^{-5} \simeq 0.03$. This prescribes $\mathrm{Card}(\mathcal{M}_n) = 33$ possible initial densities.

In Figure 5a, we consider the case where the initial density $\rho_0 : \mathbb{R} \to \mathcal{M}_5 := (2^{-5}\mathbb{N} \cap [0,1])$ is defined as follows: $\rho_0(x) = 0.9688$ for $x \in (-\infty, 10)$ and $\rho_0(x) = 0.0938$ for $x \in (10, \infty]$. Two autonomous vehicles, denoted by AV_0 and AV_1, are deployed on the road at $(0, 8)$ and $(0, 12)$, respectively ($N_1 = 0$, $N_2 = 1$ and $N = 2$). The solution (ρ, y_0, y_1) of (LWR-AVs) is

$$\rho(t,x) = \begin{cases} 0.9688 & \text{if } x \leqslant -0.9376t + 10, \\ \frac{1}{2} - (\frac{x-10}{2t}) & \text{if } -0.9376t + 10 \leqslant x \leqslant 0.8124t + 10, \\ 0.0938 & \text{if } 0.8124t + 10 \leqslant x, \end{cases}$$

and

$$y_0(t) \approx \begin{cases} 0.0312t + 10 & \text{if } t \leqslant 2.06, \\ 10 + t - 2.78\sqrt{t} & \text{if } 2.06 \leqslant t \leqslant 220.22, \\ 0.9062t - 10.60 & \text{if } 220.22 \leqslant t, \end{cases} \quad \text{and } y_1(t) = 0.9062t + 10.$$

Using the on-board sensors on the AVs, we observe $\rho(\cdot, y_0(\cdot)\pm)$ and $\rho(\cdot, y_1(\cdot)\pm)$. From Theorem 3.2, $T_0 \approx 240.93$. Using Lemma 3.5, we can reconstruct the density $\rho(220.22, \cdot)$ over $[y_0(220.22), y_1(220.22)]$. To solve numerically (LWR-AVs) with initial density ρ_0, we use the wave-front tracking method described in subsection 4.1.1 with $n = 5$. The trajectories of the autonomous vehicles are plotted in black in Figure 5a and Figure 5b. In Figure 5b, we reconstruct traffic state using two AVs over the first 20 seconds. Since we don't observe enough time ($20 < 220.22$), we notice that the reconstructed traffic state is not the true traffic state.

In Figure 6, we consider the example of two shocks with a fan of rarefaction shocks between the two shocks. A total of three AVs, denoted by AV_0, AV_1 and AV_2, are used to reconstruct the traffic state (resulting in two regions of reconstruction between AV_0 and AV_1, and between AV_1 and AV_2). Specifically, the initial density ρ_0 is defined as follows: $\rho_0(x) = 0.0938$ for $x \in (-\infty, 8]$, $\rho_0(x) = 0.9062$ for $x \in (8, 10]$, $\rho_0(x) = 0.2188$ for $x \in (10, 13]$ and $\rho_0(x) = 0.9062$ for $x \in (13, \infty)$. AV_0, AV_1, and AV_2 start at $x = 5$, $x = 9$, and $x = 12$, respectively. The resulting traffic state solved using wave front tracking over the first 20 seconds is shown in Figure 6a, while the reconstructed state between the AVs is shown in Figure 6b. The time at which the reconstruction becomes valid is $T_0 = 6.87$ between AV_0 and AV_1, and $T_1 = 3.39$ between AV_1 and AV_2.

In Figure 7, a total of four AVs, denoted by AV_0, AV_1, AV_2 and AV_3, are used to reconstruct the traffic state ($N_1 = 0$, $N_2 = 1$ and $N = 2$). The initial density ρ_0 is defined as follows: $\rho_0(x) = 0.0938$ for $x \in (-\infty, 2.1)$, $\rho_0(x) = 0.9688$ for $x \in [2.1, 10.1)$, $\rho_0(x) = 0.2500$ for $x \in [10.1, 12)$, $\rho_0(x) = 0.4375$ for $x \in [12, 16)$, $\rho_0(x) = 0.7812$ for $x \in [16, 19)$, and $\rho_0(x) = 0.9688$ for $x \in [19, \infty)$. The initial positions of AV_0, AV_1, AV_2, and AV_3 are 4, 8, 12 and 17.5, respectively. The time at which a reconstruction is found is $T_0 = 5.12$ between AV_0 and AV_1, $T_1 = 12.45$ between AV_1 and AV_2, and $T_2 = 0.00$ between AV_2 and AV_3.

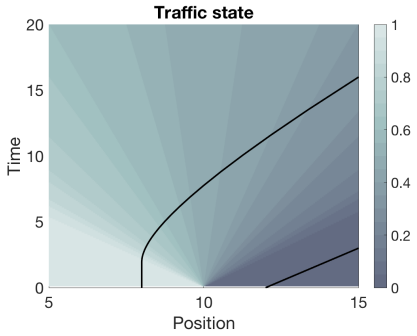

(a) True state over the first 20 seconds solved using wave front tracking.

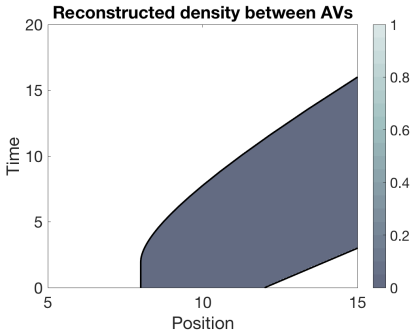

(b) Reconstructed traffic state using two AVs over the first 20 seconds.

Fig. 5: Traffic state reconstruction with two autonomous vehicles starting at $x = 8$ and $x = 12$ with initial density defined as follows: $\rho_0(x) = 0.9688$ for $x \in (-\infty, 10)$ and $\rho_0(x) = 0.0938$ for $x \in (10, \infty]$.

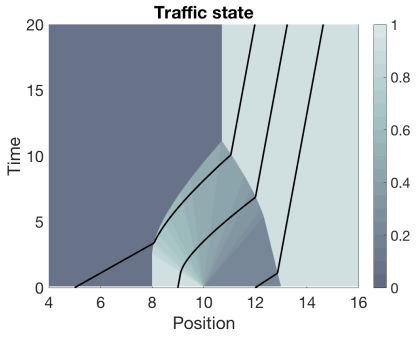

(a) True state over the first 20 seconds solved using wave front tracking.

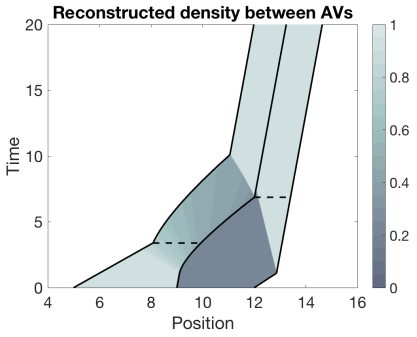

(b) Reconstructed traffic state using three AVs over the first 20 seconds.

Fig. 6: Example comparison of the true state solved using wave front tracking and the reconstructed state reconstructed using three AVs starting at $x = 5$, $x = 9$ and $x = 12$. The initial density ρ_0 is defined as follows: $\rho_0(x) = 0.0938$ for $x \in (-\infty, 8]$, $\rho_0(x) = 0.9062$ for $x \in (8, 10]$, $\rho_0(x) = 0.2188$ for $x \in (10, 13]$ and $\rho_0(x) = 0.9062$ for $x \in (13, \infty)$. Note that the reconstruction is exact and thus there is no error between the reconstructed density and the true density after time T.

In Figure 8, AV_{-2}, AV_{-1} and AV_0 starts respectively at $(t_{-2}, y_0^{-2}) = (6, 0)$, $(t_{-1}, y_0^{-1}) = (1, 0)$ and $(t_0, y_0^0) = (0, 8)$ ($N_1 = 2$, $N_2 = 0$,$N = 3$). The initial density ρ_0 is defined as follows: $\rho_0(x) = 0.3125$ for $x \in (-\infty, -1]$, $\rho_0(x) = 0.5$ for $x \in [-1, 4]$, $\rho_0(x) = 0.8125$ for $x \in [4, 10]$, and $\rho_0(x) = 0.5$ for $x \in (10, \infty)$. Thus, AV_{-2} and AV_{-1} start after AV_0 is already driving. The times at which the state can be reconstructed is $T_{-2} = 8.615$ for the state between AV_{-2} and AV_{-1}, and $T_{-1} = 5.538$ between the AV_{-1} and AV_0.

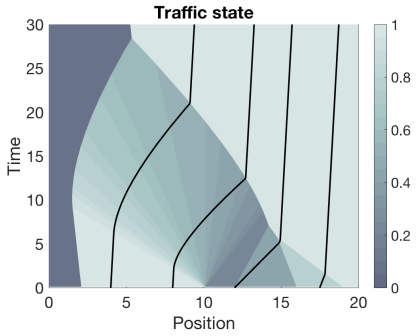

(a) True state over the first 30 seconds solved using wave front tracking.

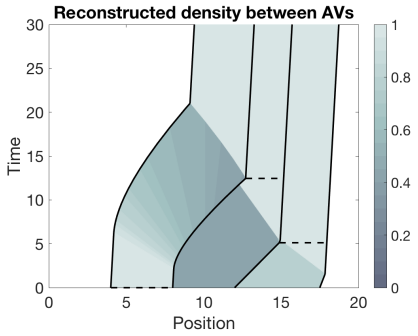

(b) Reconstructed traffic state using four AVs over the first 30 seconds.

Fig. 7: Example comparison of the true state solved using wave front tracking and the reconstructed state reconstructed using four AVs starting at $x = 4, 8, 12$ and $x = 17.5$. The reconstruction is exact and thus there is no error between the reconstructed density and the true density after time T.

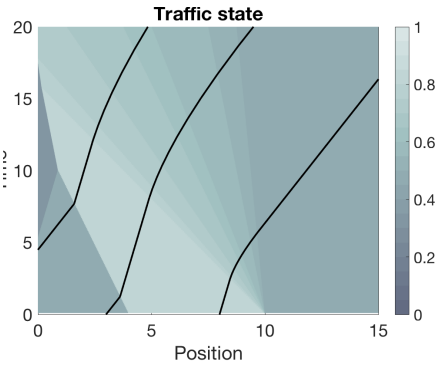

(a) True state over the first 20 seconds solved using wave front tracking.

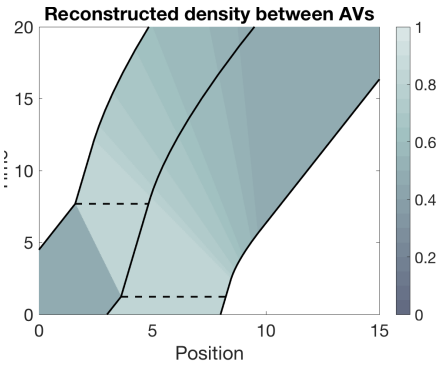

(b) Reconstructed traffic state using two AVs over the first 20 seconds.

Fig. 8: Traffic state reconstruction with three autonomous vehicles starting at $(t_{-2}, y_0^{-2}) = (6, 0)$, $(t_{-1}, y_0^{-1}) = (1, 0)$ and $(t_0, y_0^0) = (0, 8)$. The initial density ρ_0 is defined as follows: $\rho_0(x) = 0.3125$ for $x \in (-\infty, -1]$, $\rho_0(x) = 0.5$ for $x \in [-1, 4]$, $\rho_0(x) = 0.8125$ for $x \in [4, 10]$, and $\rho_0(x) = 0.5$ for $x \in (10, \infty)$. The reconstruction is exact and thus there is no error between the reconstructed density and the true density after time T.

In Figure 9, one autonomous vehicle, denoted by AV_0, is deployed on a ring ($M = 1$ in subsection 3.1). The initial density ρ_0 is a 10-periodic function defined as follows: $\rho_0(x) = 0.8125$ for $x \in (0, 2)$, $\rho_0(x) = 0.3125$ for $x \in (2, 10)$. Since ρ and y_0 are also 10 periodic functions, both trajectories plotted in black in Figure 9b are the ones of AV_0. The traffic state on the whole ring can be reconstructed after

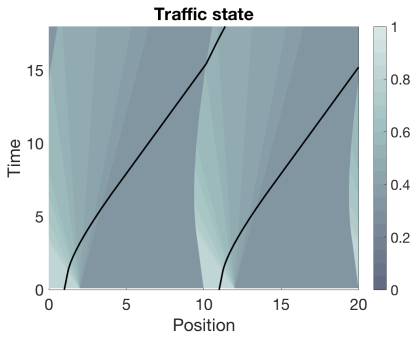

(a) True state over the first 18 seconds solved using wave front tracking.

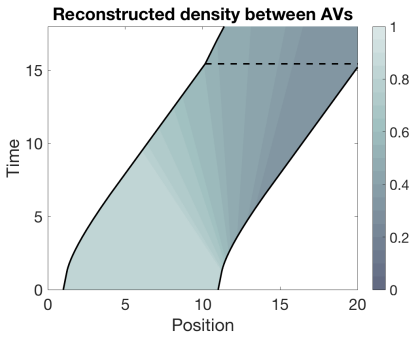

(b) Reconstructed traffic state using one AV over the first 18 seconds.

Fig. 9: Traffic state reconstruction with one autonomous vehicles on a ring of length 10 with a 10-periodic initial density defined as follows: $\rho_0(x) = 0.8125$ for $x \in (0, 2)$, $\rho_0(x) = 0.3125$ for $x \in (2, 10)$. The reconstruction is exact and thus there is no error between the reconstructed density and the true density after time T.

.

$T_{\max} = 15.444$.

6. Conclusions. The main result of this work is the theoretical analysis and a numerical scheme to reconstruct the bulk traffic density using only data along the trajectory of a small number of autonomous vehicles. The results are derived for the case when the bulk flow is described by LWR-type traffic flow models. Moving forward, there are several interesting extensions of the present work. For example, we are also interested in using AVs to estimate the traffic in and around phantom traffic jams [24], which are jams that seemingly appear without a cause but are due to human driving behavior. These jams are particularly challenging to track on real freeways due to the space and timescale on which they are found. Extending the methods developed in the present article to bulk flow models (e.g., [12]) that are able to reproduce these waves is a promising direction. Other directions include extension of the developed methods to traffic flow networks and testing of the algorithm on empirical traffic data collected from the field.

Appendix A. Proof of Theorem 3.2, Theorem 3.3, Lemma 3.5 and Theorem 3.6. In order to simplify the notations, we introduce the function $g_i : [t_i, +\infty) \to [0, 1]$ in

$$g_i(t+) := \lim_{x \to y_i(t), y_i(t) < x} \rho(t, x) = \rho(t, y_i(t)+)$$

and

$$g_i(t-) := \lim_{x \to y_i(t), x < y_i(t)} \rho(t, x) = \rho(\cdot, y_i(\cdot)-),$$

where $(\rho(t, y_i(t)\pm))_{i \in \{-N_1, \cdots, N_2\}} = \Gamma(\bar{\rho}_0)$. Since the speed of the AV is faster than (or equal to) the speed of every discontinuity, the function g_i is well-defined.

We recall that the i^{th} autonomous vehicle starts at time t_i in the position y_0^i. If $i \in \{-N_1, \cdots, -1\}$, $y_i^0 = \alpha$ and $t_i > 0$ and if $i \in \{0, \cdots, N_2\}$, $\alpha \leqslant y_i^0$ and $t_i = 0$.

A.1. Generalized characteristics. The proofs of Theorem 3.2, Theorem 3.3 and Lemma 3.5 are based on the concept of generalized characteristic (see [7, Chapter XI]). A generalized characteristic $\xi(\cdot)$ is a Lipschitz curve, defined on the time interval $[\sigma,\tau]\subset[0,\infty)$ associated with the solution ρ, verifying for almost all $t\in[\sigma,\tau]$,

(A.1)
$$\dot\xi(t)=\begin{cases} f'(\rho(t,\xi(t))) & \text{when } \rho(t,\xi(t)+)=\rho(t,\xi(t)-)=\rho(t,\xi(t)),\\ \frac{f(\rho(t,\xi(t)+))-f(\rho(t,\xi(t)-))}{\rho(t,\xi(t)+)-\rho(t,\xi(t)-)} & \text{when } \rho(t,\xi(t)-)<\rho(t,\xi(t)+).\end{cases}$$

Let $\bar t>0$. We denote by $\xi_-(\cdot,\bar t,\bar x)$ and $\xi_+(\cdot,\bar t,\bar x)$ the minimal and maximal backward characteristics, associated with an admissible solution ρ, coming from a point $(\bar t,\bar x)$. From [7, Thm 10.3.1, Thm 11.1.3], we have, for every $i\in\{-N_1,\cdots,N_2\}$,

(A.2)
$$\begin{cases} \xi_-(t,\bar t,y_i(\bar t))=\xi_+(t,\bar t,y_i(\bar t))=f'(g_i(\bar t))(t-\bar t)+y_i(\bar t) & \text{when } g_i(\bar t-)=g_i(\bar t+)\\ \left.\begin{aligned}\xi_-(t,\bar t,y_i(\bar t))&=f'(g_i(\bar t-))(t-\bar t)+y_i(\bar t)\\ \xi_+(t,\bar t,y_i(\bar t))&=f'(g_i(\bar t+))(t-\bar t)+y_i(\bar t)\end{aligned}\right| & \text{when } g_i(\bar t-)<g_i(\bar t+).\end{cases}$$

The next Lemma gives the domain of dependence of (LWR) for a point $(t,x)\in\mathbb{R}_+\times\mathbb{R}$ (see [7, Theorem 10.2.2]).

LEMMA A.1. *Let $i\in\{-N_1,\cdots,N_2\}$, $\rho_0\in L^1(\mathbb{R})\cap BV(\mathbb{R},[0,1])$ and $(t,x)\in(t_i,\infty)\times[y_0^i,\infty)$. The value $S_t(\rho_0)(x):=\rho(t,x)$ depends only on values of $\rho(\cdot,\cdot)$ in the subset $\{(s,y)\in[0,t]\times\mathbb{R}/\xi_-(s,t,x)\leqslant y\leqslant\xi_+(s,t,x)\}\cap\{(s,y)\in[0,t]\times\mathbb{R}/y_0^i\leqslant y\}$ of $\mathbb{R}^2$.*

A.2. Some properties of φ_i. First of all, using (A.2), φ_i defined in (3.1) can be rewritten as follows:

$$\varphi_i:t\to[\xi_-(t_{i+1},t,y_i(t)),\xi_+(t_{i+1},t,y_i(t))]. \tag{A.3}$$

LEMMA A.2. *φ_i is an increasing application over $[t_i,\infty]$ in the following sense: for every $t_i\leqslant t_1<t_2$,*

$$f'(g_i(t_1+))(t_{i+1}-t_1)+y_i(t_1)\leqslant f'(g_i(t_2-))(t_{i+1}-t_2)+y_i(t_2).$$

Proof. Let $t_i\leqslant t_1<t_2$. If $\xi_+(\cdot,t_1,y_i(t_1))$ and $\xi_-(\cdot,t_2,y_i(t_2))$ coincide over $[t_i,t_1]$ then, from (A.2),

$$f'(g_i(t_1+))(t_{i+1}-t_1)+y_i(t_1)=f'(g_i(t_2-))(t_{i+1}-t_2)+y_i(t_2).$$

Otherwise, since $\xi_+(\cdot,t_1,y_i(t_1))$ and $\xi_-(\cdot,t_2,y_i(t_2))$ are shock-free[1], from [7, Corollary 11.1.2], $\xi_+(\cdot,t_1,y_i(t_1))$ and $\xi_-(\cdot,t_2,y_i(t_2))$ cannot interact for any $t\in(0,t_1]$. Moreover, using that $u_i(\rho)\geqslant f'(\rho)$ for every $\rho\in[0,1]$, we have $\xi_+(t,t_1,y_i(t_1))\leqslant\xi_-(t,t_2,y_i(t_2))$ for every $t\in[t_{i+1},t_1]$. In particular, we obtain $\xi_+(t_{i+1},t_1,y_i(t_1))\leqslant\xi_-(t_{i+1},t_2,y_i(t_2))$. From (A.2), we deduce that if $t_i\leqslant t_1<t_2$ then
$f'(g_i(t_1+))(t_{i+1}-t_1)+y_i(t_1)\leqslant f'(g_i(t_2-))(t_{i+1}-t_2)+y_i(t_2)$.

LEMMA A.3. *Let $0<\rho_{\min}\leqslant\bar\rho_0(\cdot)\leqslant\rho_{\max}$ and $c_i:=\min_{\rho\in[\rho_{\min},\rho_{\max}]}(u_i(\rho)-f'(\rho))>0$.*

[1] A generalized characteristic $\xi(\cdot)$, associated with ρ and defined on $[\sigma,\tau]$, is called shock-free if $\rho(\xi(t)-,t)=\rho(\xi(t)+,t)$, for almost all t in $[\sigma,\tau]$.

- *Let $t_0 > 0$. Assuming that $g_i'(\cdot)$ is well-defined over (t_0, t_1) and $g_i'(t) < 0$ for every $t \in (t_0, t_1)$ then*

$$t_1 \leqslant t_0 \exp\left(\frac{f'(g_i(t_1-)) - f'(g_i(t_0+))}{c_i}\right). \tag{A.4}$$

- *Assuming that $g_i(\cdot)$ is an increasing function over (t_0, t_1) then, for every $x_1 \in \varphi_i(t_1)$ and $x_0 \in \varphi_i(t_0)$,*

$$x_1 - x_0 \geqslant c_i(t_1 - t_0).$$

- *If $g_i(t_0-) < g_i(t_0+)$ then*

$$\lambda(\varphi_i(t_0)) = (f'(g_i(t_0+)) - f'(g_i(t_0-)))(t_{i+1} - t_0),$$

where λ denotes the Lebesgue measure.

Proof.

- Since $g_i'(t) < 0$ for every $t \in (t_0, t_1)$, then there exists $x_r \in R$ such that $g_i(t) = (f')^{-1}(\frac{y_1(t)-x_r}{t})$ for every $t \in (t_0, t_1)$. Thus, y_i verifies

$$\begin{cases} \dot{y}_i(t) = u_i((f')^{-1}(\frac{y_1(t)-x_r}{t})), & t_0 < t \leqslant t_1, \\ y_i(t_0) = x_0. \end{cases}$$

  Above, x_r is the starting point of the rarefaction wave crossed by the i^{th} autonomous vehicle over (t_0, t_1). Let $\tilde{y}_i(\cdot)$ defined by

$$\begin{cases} \dot{\tilde{y}}_i(t) = \frac{\tilde{y}_i(t)-x_r}{t} + c_i, & t > t_0, \\ \tilde{y}_i(t_0) = x_0. \end{cases} \tag{A.5}$$

  Since $u_i(\rho) \geqslant f'(\rho) + c_i$, we have $\tilde{y}_i(t) \leqslant y_i(t)$ for every $t \in [t_0, t_1]$. In particular, $\tilde{y}_i(t_1) \leqslant y_i(t_1) = f'(g_i(t_1-))t_1 + x_r$. From (A.5), for every $t \geqslant t_0$, $\tilde{y}_i(t) = c_i t \ln(\frac{t}{t_0}) + x_r + tf'(g_1(t_0+))$. Thus, we have

$$t_1 \leqslant t_0 \exp\left(\frac{f'(g_i(t_1-)) - f'(g_i(t_0+))}{c_i}\right),$$

  whence the conclusion of (A.4). ∎

- Let $x_1 \in \varphi_i(t_1)$ and $x_0 \in \varphi_i(t_0)$. By definition of φ_i in (3.1) and using that y_i is solution of (2.4), we have

$$\begin{aligned} x_1 - x_0 &\geqslant f'(g_i(t_1-))(t_{i+1} - t_1) + y_i(t_1) - f'(g_i(t_0+))(t_{i+1} - t_0) - y_i(t_0), \\ &\geqslant f'(g_i(t_1-))(t_{i+1} - t_1) - f'(g_i(t_0+))(t_{i+1} - t_0) + \textstyle\int_{t_0}^{t_1} u_i(g_i(s))\, ds \end{aligned}$$

  Since $g_i(\cdot)$ is an increasing function over (t_0, t_1) and $u_i(\rho) \geqslant f'(\rho) + c_i$ for every $\rho \in [\rho_{\min}, \rho_{\max}]$,

$$\begin{aligned} x_1 - x_0 &\geqslant f'(g_i(t_1-))(t_{i+1} - t_1) - f'(g_i(t_0+))(t_{i+1} - t_0) \\ &\quad + f'(g_i(t_1-))(t_1 - t_0) + c_i(t_1 - t_0) \\ &\geqslant (f'(g_i(t_1-)) - f'(g_i(t_0+)))(t_{i+1} - t_0) + c_i(t_1 - t_0). \end{aligned}$$

  Using that $f'(g_i(t_1-)) - f'(g_i(t_0+)) \leqslant 0$ and $t_{i+1} - t_0 \leqslant 0$, we conclude that

$$x_1 - x_0 \geqslant c_i(t_1 - t_0).$$

- We have

$$\begin{aligned} \lambda(\varphi_i(t_0)) &= f'(g_i(t_0+))(t_{i+1} - t_0) + y_i(t_0) - f'(g_i(t_0-))(t_{i+1} - t_0) \\ &\quad + y_i(t_0) \\ &= (f'(g_i(t_0+)) - f'(g_i(t_0-)))(t_{i+1} - t_0). \end{aligned}$$

A.3. Proof of Theorem 3.2. Let $\rho_0 \in L^1(\mathbb{R}) \times BV(\mathbb{R}, [0,1])$, $i \in \{-N_1, \cdots, N_2 - 1\}$ and $x \in (y_i(T_i), y_{i+1}(T_i))$.

Since T_i verifies (3.2) and using that $T_i < +\infty$ with (A.2), we have

$$y_0^{i+1} \in [\xi_-(t_{i+1}, T_i, y(T_i)), \xi_+(t_{i+1}, T_i, y(T_i))]. \tag{A.6}$$

Above, $\xi_-(\cdot, T_i, y(T_i))$ and $\xi_+(\cdot, T_i, y(T_i))$ are the minimal and maximal backward characteristics respectively, associated with ρ_0, coming from the point $(T_i, y(T_i))$. Using that $y_i(T_i) < x$ and since T_i verifies (3.2) we have

$$\xi_+(t_{i+1}, T_i, y(T_i)) < \xi_+(t_{i+1}, T_i, x) \tag{A.7}$$

From (A.6) and (A.7), we conclude that $y_0^{i+1} < \xi_-(t_{i+1}, T_i, x)$. and since $u_{i+1}(\rho) \geqslant f'(\rho)$, $\xi_-(\cdot, T_i, x)$ (resp. $\xi_+(\cdot, T_i, x)$) interacts only once at time $t_- \geqslant t_{i+1}$ (resp. at time $t_+ \geqslant t_{i+1}$) with $y_{i+1}(\cdot)$. Thus, $S_{T_i}(\rho_0)(x)$ depends only on $\{S_t(\rho_0)(y_{i+1}(t)), t \in [t_-, t_+]\}$. Since, for every $\rho_0 \in \Gamma^{-1}(\Gamma(\bar\rho_0))$ and for every $t \in \mathbb{R}_+$, $S_t(\rho_0)(y_{i+1}(t)) = S_t(\bar\rho_0)(y_{i+1}(t))$, we have

$$S_{T_i}(\rho_0)(x) = S_{T_i}(\bar\rho_0)(x).$$

A.4. Proof of Theorem 3.3. Since, for every $x \in \mathbb{R}$, $0 < \rho_{\min} \leqslant \bar\rho_0(x) \leqslant \rho_{\max}$, we have $\rho_{\min} \leqslant g_i(t) \leqslant \rho_{\max}$ for every $i \in \{-N_1, \cdots, N_2\}$. Thus, for every $t \geqslant t_i$,

$$\varphi_i(t) \subset [(t - t_{i+1})(u_i(\rho_{\max}) - f'(\rho_{\min})) + y_0^i, (t - t_{i+1})(u_i(\rho_{\min}) - f'(\rho_{\max})) + y_0^i].$$

Since $u_i(\rho) \geqslant f'(\rho)$, for every $\rho \in [0,1]$, we have $u_i(\rho_{\min}) - f'(\rho_{\max}) \geqslant 0$ and we conclude that

$$T_i \geqslant \frac{y_0^{i+1} - y_0^i}{u_i(\rho_{\min}) - f'(\rho_{\max})} + t_{i+1}.$$

Since the quantity $u_i(\rho_{\max}) - f'(\rho_{\min})$ may be negative, finding an upper bound of T_i is not as straightforward as before. Using $TV(\bar\rho_0) < \infty$, there exists $(\bar t_{2k+1})_{k \in \{0, \cdots, N\}}$ such that $g_i(\cdot)$ is a non-increasing function over $\cup_{k=0}^N (\bar t_{2k+1}, \bar t_{2k+2})$ with $N \in \mathbb{N} \cup \{\infty\}$ and $g_i(\cdot)$ is an increasing function over $\mathbb{R} \backslash \{\cup_{k=0}^N (\bar t_{2k+1}, \bar t_{2k+2})\}$. For every $k \in \{0, \cdots, N+1\}$, $\bar t_{2k+1} \geqslant t_i$ and since y_i is solution of (2.4), we have $\bar t_1 > 0$. We introduce the set $\mathcal{I} \subset \mathbb{N} \cup \{\infty\}$ defined by

$$\mathcal{I} = \left\{ k \in \mathbb{N} \cup \{\infty\} / \xi_+(t_{i+1}, \bar t_{2k+1}, y_i(\bar t_{2k+1})) = \xi_-(t_{i+1}, \bar t_{2k+2}, y_i(\bar t_{2k+2})) \leqslant y_0^{i+1} \right\}.$$

Using (A.4), for every $k \in \mathbb{N}$, we have

$$\begin{cases} \bar t_{2k+2} \leqslant \bar t_{2k+1} \exp\left(\frac{f'(g_i(\bar t_{2k+2}-)) - f'(g_i(\bar t_{2k+1}+))}{c_i} \right), \\ \bar t_{2k} \leqslant \bar t_{2k-1} \exp\left(\frac{f'(g_i(\bar t_{2k}-)) - f'(g_i(\bar t_{2k-1}+))}{c_i} \right). \end{cases} \tag{A.8}$$

If $\bar t_{2k+1} = \bar t_{2k}$, from (A.8), we have immediately that

$$\bar t_{2k+2} \leqslant \bar t_{2k-1} \exp\left(\frac{f'(g_i(\bar t_{2k+2}-)) - f'(g_i(\bar t_{2k+1}+)) + f'(g_i(\bar t_{2k}-)) - f'(g_i(\bar t_{2k-1}+))}{c_i} \right). \tag{A.9}$$

Otherwise,

$$\begin{aligned} \bar t_{2k+2} \leqslant \quad & \exp\left(\frac{f'(g_i(\bar t_{2k+2}-)) - f'(g_i(\bar t_{2k+1}+))}{c_i} \right) \cdot \\ & \cdot \left(\bar t_{2k+1} - \bar t_{2k} + \bar t_{2k-1} \exp\left(\frac{f'(g_i(\bar t_{2k}-)) - f'(g_i(\bar t_{2k-1}+))}{c_i} \right) \right). \end{aligned} \tag{A.10}$$

Since, for every $k \in \mathbb{N}$,
$f'(g_i(\bar{t}_{2k+2}-)) - f'(g_i(\bar{t}_{2k+1}+)) \leqslant \alpha(g_i(\bar{t}_{2k+1}+) - g_i(\bar{t}_{2k+2}-))$ with
$\alpha = \sup_{\rho\in[\rho_{\min},\rho_{\max}]} f''(\rho)$, we have, for every $p \in \{0,\cdots,k\}$,

$$\sum_{j=p}^{k} \frac{f'(g_i(\bar{t}_{2j+2}-)) - f'(g_i(\bar{t}_{2j+1}+))}{c_i} \leqslant \frac{\alpha TV(\bar{\rho}_0)}{c_i}. \tag{A.11}$$

We introduce $A(k) = \{j \in \{0,\cdots,k\}/\bar{t}_{2j+1} \neq \bar{t}_{2j}\}$. Using (A.9), (A.10) and (A.11), by induction we obtain, for every $k \in \mathbb{N}$,

$$\bar{t}_{2k+2} \leqslant \left(\sum_{j\in A(k)} (\bar{t}_{2j+1} - \bar{t}_{2j})\right) \exp\left(\frac{\alpha TV(\bar{\rho}_0)}{c_i}\right). \tag{A.12}$$

Above, $\bar{t}_0 := 0$, $\bar{t}_1 \geqslant t_i$ and $\bar{t}_1 > 0$.

- If $t_i = 0$; we have immediately that $t_{i+1} = 0$. For every $j \in A(k)$, for every $t \in (\bar{t}_{2j}, \bar{t}_{2j+1})$, $g_i(\cdot)$ is an increasing function, using Lemma A.3, we have, for every $x_{2j} \in \varphi_i(\bar{t}_{2j})$ and for every $x_{2j+1} \in \varphi_i(\bar{t}_{2j+1})$,

  $$x_{2j+1} - x_{2j} \geqslant c_i(\bar{t}_{2j+1} - \bar{t}_{2j}). \tag{A.13}$$

  Since $\bar{t}_1 > 0$ and $\bar{t}_0 := 0$, we have $0 \in A(k)$ and $\varphi_i(0+) = \{y_0^i\}$. Since $k \in \mathcal{I}$, for every $x_{2k+1} \in \varphi(\bar{t}_{2k+1})$, $x_{2k+1} \leqslant y_0^{i+1}$. Using that, by Lemma A.2, φ_i is an increasing function and (A.13), we conclude that

  $$\sum_{j\in A(k)} (\bar{t}_{2j+1} - \bar{t}_{2j}) \leqslant \frac{y_0^{i+1} - y_0^i}{c_i}. \tag{A.14}$$

- If $t_i \neq 0$; by definition of φ_i in (3.1) and using that $0 < \rho_{\min} \leqslant \bar{\rho}_0(x) \leqslant \rho_{\max}$, for every $x \in \varphi_i(t_i+)$, $x \geqslant f'(\rho_{\min})(t_{i+1} - t_i) + y_0^{i+1}$. Since $k \in \mathcal{I}$, for every $x_{2k+1} \in \varphi(\bar{t}_{2k+1})$, $x_{2k+1} \leqslant y_0^{i+1}$. Using that, by Lemma A.2, φ_i is an increasing function, we conclude that

  $$\sum_{j\in A(k)} (\bar{t}_{2j+1} - \bar{t}_{2j}) \leqslant \frac{y_0^{i+1} - y_0^i + f'(\rho_{\min})(t_i - t_{i+1})}{c_i}. \tag{A.15}$$

Combining (A.12) with (A.15), we have, for every $i \in \mathbb{N}^*$,

$$t_{2k+2} \leqslant \frac{(y_0^{i+1} - y_0^i + f'(\rho_{\min})(t_i - t_{i+1}))\exp(\frac{\alpha TV(\bar{\rho}_0)}{c_i})}{c_i} < +\infty. \tag{A.16}$$

- If $\mathrm{Card}(\mathcal{I}) < \infty$; we have $T_i \in [t_{2\mathrm{Card}(\mathcal{I})+2}, t_{2\mathrm{Card}(\mathcal{I})+3}]$ and $g_i(\cdot)$ is an increasing function over $(t_{2\mathrm{Card}(\mathcal{I})+2}, t_{2\mathrm{Card}(\mathcal{I})+3})$. We notice that $t_{2\mathrm{Card}(\mathcal{I})+3}$ may be infinite. Thus, from Lemma A.3, we deduce that

  $$T_i - t_{2\mathrm{Card}(\mathcal{I})+2} \leqslant \frac{(y_0^{i+1} - (f'(\rho_{\min})(t_{i+1} - t_i) + y_0^i))}{c_i}.$$

  Using (A.16), we conclude that

  $$T_i \leqslant \frac{(y_0^{i+1} - y_0^i + f'(\rho_{\min})(t_i - t_{i+1}))}{c_i}\left(1 + \exp\left(\frac{\alpha TV(\bar{\rho}_0)}{c_i}\right)\right).$$

- If $\mathrm{Card}(\mathcal{I}) = \infty$; from (A.16), the increasing sequence $\{t_{2k+2}\}_{k\in\mathcal{I}}$ is bounded. Thus, there exists $t_\infty (\geqslant t_i)$ such that $\lim_{k\to\infty} t_{2k+2} = t_\infty$.
  From Lemma A.3, we deduce that

$$T_i - t_\infty \leqslant \frac{(y_0^{i+1} - y_0^i + f'(\rho_{\min})(t_i - t_{i+1}))}{c_i}.$$

  Using (A.16), we conclude that

$$T_i \leqslant \frac{(y_0^{i+1} - y_0^i + f'(\rho_{\min})(t_i - t_{i+1}))}{c_i}\left(1 + \exp\left(\frac{\alpha TV(\bar\rho_0)}{c_i}\right)\right).$$

A.5. Proof of Lemma 3.5. Let $\rho_0 \in L^1(\mathbb{R})\times BV(\mathbb{R},[0,1])$, $i \in \{-N_1,\cdots,N_2-1\}$ and $x \in (y_i(a), y_{i+1}(a))$. Since $g_i(\cdot) := \rho(\cdot, y_i(\cdot))$ is a constant function over $[a,b)$ and $T_i \in [a,b)$ we have, for every $t \in [t_{i+1}, T_i]$,

$$f'(g_i(T_i)-)(t-t_i) + y_i(T_i) = f'(g_i(T_i)+)(t-T_i) + y_i(T_i).$$

By definition of T_i in (3.2), if $x > f'(g_i(T_i))(a-T_i) + y_i(T_i)$, $S_a(\rho_0)(x)$ only depends on $\{S_t(\rho_0)(y_{i+1}(t)), t \in [t_{i+1},\infty]\}$. If $y_i(a) \leqslant x \leqslant f'(g_i(T_i))(a-T_i) + y_i(T_i)$, since g_i is a constant function over $[a,b)$ and $u_i(\rho) \geqslant f'(\rho)$ for every $\rho \in [0,1]$, no waves can interact with the straight line passing through $(a, y_i(a))$ and $(T_i, y_i(T_i))$ and therefore with the straight line passing through $(a, y_i(a))$ and $(a, f'(g_i(T_i))(a-T_i)+y_i(T_i))$. We conclude that $S_a(\rho_0)(x)$ depends only on $\{S_t(\rho_0)(y_{i+1}(t)), t \in [t_{i+1},+\infty)\}$. Since, for every $\rho_0 \in \Gamma^{-1}(\Gamma(\bar\rho_0))$ and for every $t \in [t_{i+1},+\infty)$, $S_t(\rho_0)(y_{i+1}(t)) = S_t(\bar\rho_0)(y_{i+1}(t))$, we have

$$S_a(\rho_0)(x) = S_a(\bar\rho_0)(x).$$

A.6. Proof of Theorem 3.6. Consider the following PDE-ODE system

$$\text{(A.17)}\qquad \begin{cases} \partial_t\tilde\rho + \partial_x(f(\tilde\rho)) = 0, & (t,x) \in \mathbb{R}^+\times\mathbb{R},\\ \tilde\rho(0,x) = \bar\rho_0(x), & x\in\mathbb{R},\\ \dot{\tilde y}_i(t) = u_i(\tilde\rho(t,\tilde y_i(t)+))), & t\in\mathbb{R}^+, i = 1,\cdots,M\\ \tilde y_i(0) = y_0^i, & i = 1,\cdots,M \end{cases}$$

where $(y_0^i)_{i=1,\cdots,M} \in [0,L]^M$ are the initial positions of the M autonomous vehicles. We add a $(M+1)^{\text{th}}$ autonomous vehicle defined as follows:

$$\text{(A.18)}\qquad \begin{cases} \dot{\tilde y}_{M+1}(t) = u_{M+1}(\tilde\rho(t,\tilde y_{M+1}(t)+))), & t\in\mathbb{R}^+\\ \tilde y_{M+1}(0) = y_0^{M+1}, \end{cases}$$

with $y_0^{M+1} = y_1^0 + L$ and $u_{M+1} = u_1$. Since ρ is solution of (3.4) and $\tilde\rho$ is solution of (A.17), we have immediately the following Lemma.

LEMMA A.4. *Let $t \in \mathbb{R}_+$ and $i \in \{1,\cdots,M\}$, $k \in \mathbb{N}$.*

- *If $kL \leqslant \tilde y_i(t) < (k+1)L$ and $kL \leqslant \tilde y_{i+1}(t) < (k+1)L$, we have $\tilde y_i(t) = y_i(t) + kL$ and $\tilde y_{i+1}(t) = y_{i+1}(t) + kL$. Moreover, for every $x \in [\tilde y_i(t), \tilde y_{i+1}(t)]$*

$$\tilde\rho(t,x) = \rho(t, x-kL).$$

- *If $kL \leqslant \tilde y_i(t) < (k+1)L$ and $(k+1)L \leqslant \tilde y_{i+1}(t) < (k+2)L$, we have $\tilde y_i(t) = y_i(t) + kL$ and $\tilde y_{i+1}(t) = y_{i+1}(t) + (k+1)L$. Moreover,*

$$\tilde\rho(t,x) = \begin{cases} \rho(t,x-kL) & \forall x \in [\tilde y_i(t), (k+1)L]\\ \rho(t,x-(k+1)L) & \forall x \in [(k+1)L, \tilde y_{i+1}(t)]. \end{cases}$$

For every $i \in \{1, \cdots, M\}$, we define $\tilde{T}_i \in \mathbb{R} \cup \{+\infty\}$ as in (3.2) with

$$\varphi_i(t) = [f'(\tilde{\rho}(t, \tilde{y}_i(t)-))(t_{i+1} - t) + \tilde{y}_i(t), f'(\tilde{\rho}(t, \tilde{y}_i(t)+))(t_{i+1} - t) + \tilde{y}_i(t)].$$

Since for every $i \in \{0, \cdots, M\}$ $y_0^{i+1} - y_0^i \leqslant L$ and $\tilde{\rho}_0$ is a L-periodic function verifying that $\tilde{\rho}_0 = \bar{\rho}_0$ over $[0, L]$, we have $TV(\rho(\cdot, \tilde{y}_i(\cdot)), [0, \tilde{T}_i]) \leqslant TV(\rho_0)$. Mimicking the proofs of Theorem 3.2 and Theorem 3.3, we have, for every $i \in \{1, \cdots, M\}$

$$\tilde{T}_i \leqslant \frac{y_0^{i+1} - y_0^i}{c_i} \left(1 + \exp\left(\frac{\alpha TV(\rho_0)}{c_i}\right)\right), \tag{A.19}$$

and for every $\rho_0 \in \Gamma^{-1}(\Gamma(\tilde{\rho}_0))$, $\tilde{S}_{\tilde{T}_i}(\rho_0)(x) = \tilde{S}_{\tilde{T}_i}(\tilde{\rho}_0)(x)$, for every $i \in \{1, \cdots, M\}$ and for almost every $x \in [\tilde{y}_i(\tilde{T}_i), \tilde{y}_{i+1}(\tilde{T}_i)]$ with $(\tilde{y}_i, \tilde{y}_{i+1})$ solution of (A.17) and (A.18). Here, $\tilde{S}_t$ is the L^1-Lipschitz semigroup defined by $S_t(\rho_0) = \tilde{\rho}(t, \cdot)$ s.t. $\tilde{\rho}$ is the solution of (A.17). Using that $\tilde{\rho}$ is a L-periodic function such that $\tilde{\rho} = \bar{\rho}$ over $[0, L]$, Lemma A.4 and $\tilde{y}_1(t) - \tilde{y}_{M+1}(t) = L$ for every $t \in \mathbb{R}_+$, we conclude the proof of Theorem 3.6.

REFERENCES

[1] D. Amadori and R. M. Colombo, *Continuous dependence for 2× 2 conservation laws with boundary*, journal of differential equations, 138 (1997), pp. 229–266.

[2] C. Bardos, A.-Y. LeRoux, and J.-C. Nédélec, *First order quasilinear equations with boundary conditions*, Communications in partial differential equations, 4 (1979), pp. 1017–1034.

[3] S. Bianchini and L. V. Spinolo, *The boundary riemann solver coming from the real vanishing viscosity approximation*, Archive for Rational Mechanics and Analysis, 191 (2009), p. 1.

[4] A. Bressan, *Hyperbolic systems of conservation laws*, vol. 20 of Oxford Lecture Series in Mathematics and its Applications, Oxford University Press, Oxford, 2000. The one-dimensional Cauchy problem.

[5] R. M. Colombo and F. Marcellini, *A mixed ode–pde model for vehicular traffic*, Mathematical Methods in the Applied Sciences, 38 (2015), pp. 1292–1302.

[6] R. M. Colombo and A. Marson, *A hölder continuous ode related to traffic flow*, Proceedings of the Royal Society of Edinburgh Section A: Mathematics, 133 (2003), pp. 759–772.

[7] C. M. Dafermos, *Hyperbolic conservation laws in continuum physics, volume 325 of grundlehren der mathematischen wissenschaften [fundamental principles of mathematical sciences]*, 2010.

[8] M. L. Delle Monache and P. Goatin, *Scalar conservation laws with moving constraints arising in traffic flow modeling: an existence result*, Journal of Differential equations, 257 (2014), pp. 4015–4029.

[9] C. Donadello and A. Marson, *Stability of front tracking solutions to the initial and boundary value problem for systems of conservation laws*, Nonlinear Differential Equations and Applications NoDEA, 14 (2007), pp. 569–592.

[10] F. Dubois and P. Le Floch, *Boundary conditions for nonlinear hyperbolic systems of conservation laws*, Journal of Differential Equations, 71 (1988), pp. 93–122.

[11] A. Ferrara, S. Sacone, and S. Siri, *State estimation in freeway traffic systems*, in Freeway Traffic Modelling and Control, Springer, 2018, pp. 169–190.

[12] M. R. Flynn, A. R. Kasimov, J.-C. Nave, R. R. Rosales, and B. Seibold, *Self-sustained nonlinear waves in traffic flow*, Physical Review E, 79 (2009), p. 056113.

[13] M. Fountoulakis, N. Bekiaris-Liberis, C. Roncoli, I. Papamichail, and M. Papageorgiou, *Highway traffic state estimation with mixed connected and conventional vehicles: Microscopic simulation-based testing*, Transportation Research Part C: Emerging Technologies, 78 (2017), pp. 13–33.

[14] D. C. Gazis and C. H. Knapp, *On-line estimation of traffic densities from time-series of flow and speed data*, Transportation Science, 5 (1971), pp. 283–301.

[15] J. C. Herrera and A. M. Bayen, *Incorporation of lagrangian measurements in freeway traffic state estimation*, Transportation Research Part B: Methodological, 44 (2010), pp. 460–481.

[16] J. C. Herrera, D. B. Work, R. Herring, X. J. Ban, Q. Jacobson, and A. M. Bayen, *Evaluation of traffic data obtained via GPS-enabled mobile phones: The Mobile Century field experiment*, Transportation Research Part C: Emerging Technologies, 18 (2010), pp. 568–583.

[17] M. J. Lighthill and G. B. Whitham, *On kinematic waves. ii. a theory of traffic flow on long crowded roads*, Proceedings of the Royal Society of London. Series A, Mathematical and Physical Sciences, 229 (1955), pp. 317–345, http://www.jstor.org/stable/99769.

[18] L. Mihaylova, R. Boel, and A. Hegyi, *Freeway traffic estimation within particle filtering framework*, Automatica, 43 (2007), pp. 290–300.

[19] P. Richards, *Shock waves on the highway*, Operations Research, 4 (1956), pp. 42–51, https://doi.org/10.1287/opre.4.1.42, https://doi.org/10.1287/opre.4.1.42, https://arxiv.org/abs/https://doi.org/10.1287/opre.4.1.42.

[20] T. Seo, A. M. Bayen, T. Kusakabe, and Y. Asakura, *Traffic state estimation on highway: A comprehensive survey*, Annual Reviews in Control, 43 (2017), pp. 128–151.

[21] T. Seo and T. Kusakabe, *Probe vehicle-based traffic state estimation method with spacing information and conservation law*, Transportation Research Part C: Emerging Technologies, 59 (2015), pp. 391 – 403, https://doi.org/https://doi.org/10.1016/j.trc.2015.05.019, http://www.sciencedirect.com/science/article/pii/S0968090X15002132. Special Issue on International Symposium on Transportation and Traffic Theory.

[22] D. Serre, *Systems of Conservation Laws 1: Hyperbolicity, entropies, shock waves*, Cambridge University Press, 1999.

[23] D. Serre, *Systems of conservation laws. 2. geometric structures, oscillations, and initial-boundary value problems. translated from the 1996 french original by in sneddon*, 2000.

[24] Y. Sugiyama, M. Fukui, M. Kikuchi, K. Hasebe, A. Nakayama, K. Nishinari, S.-i. Tadaki, and S. Yukawa, *Traffic jams without bottlenecks-experimental evidence for the physical mechanism of the formation of a jam*, New journal of physics, 10 (2008), p. 033001.

[25] M. W. Szeto and D. C. Gazis, *Application of kalman filtering to the surveillance and control of traffic systems*, Transportation Science, 6 (1972), pp. 419–439.

[26] Y. Wang, M. Papageorgiou, and A. Messmer, *Real-time freeway traffic state estimation based on extended kalman filter: A case study*, Transportation Science, 41 (2007), pp. 167–181.

[27] D. B. Work, S. Blandin, O.-P. Tossavainen, B. Piccoli, and A. M. Bayen, *A traffic model for velocity data assimilation*, Applied Mathematics Research eXpress, 2010 (2010), pp. 1–35.

[28] Y. Yuan, J. Van Lint, R. E. Wilson, F. van Wageningen-Kessels, and S. P. Hoogendoorn, *Real-time lagrangian traffic state estimator for freeways*, IEEE Transactions on Intelligent Transportation Systems, 13 (2012), pp. 59–70.